Int J Adv Manuf Technol (2009) 45:704–713
DOI 10.1007/s00170-009-2004-0

ORIGINAL ARTICLE

Computational approach to photonic drilling of silicon carbide

Anoop N. Samant · Claus Daniel · Ron H. Chand · Craig A. Blue · Narendra B. Dahotre

Received: 9 June 2008 / Accepted: 3 March 2009 / Published online: 14 March 2009
© Springer-Verlag London Limited 2009

Abstract The ability of lasers to carry out drilling processes in silicon carbide ceramic was investigated in this study. A JK 701 pulsed Nd:YAG laser was used for drilling through the entire depth of silicon carbide plates of different thicknesses. The laser parameters were varied in different combinations for a well-controlled drilling through the entire thickness of the SiC plates. A drilling model incorporating effects of various physical phenomena such as decomposition, evaporation-induced recoil pressure, and surface tension was developed. Such comprehensive model was capable of advance prediction of the energy and time required for drilling a hole through any desired depth of material.

Keywords Nd:YAG laser · Silicon carbide · Ceramic · Drilling

1 Introduction

Laser beams are extensively used in the manufacturing industry for drilling, cutting, micromachining, welding, sintering, and marking [1]. The high density of the beam and excellent focusing characteristics of Nd:YAG lasers have made it suitable for drilling different materials [2]. Very small holes as well as holes with high aspect ratios can be drilled by lasers. As it is a noncontact process, tool wear is minimal compared to mechanical drilling and only present in the form of laser maintenance [3].

The workpiece absorbs the incident laser energy which is transformed mainly into heat. The material undergoes phase transformations when the temperature increases above decomposition temperature, decomposition products melt, and recoil forces are produced, thus generating a hole. Generation of the taper is a vital feature during the drilling operation due to the intrinsic focusing characteristic of the laser beam [4]. The diameter of the hole at entry is larger than that at the exit giving a positive taper to most of the drilled holes. Through engineering approaches such as utilization of a lens of long focal length with longer focal waist, such a taper can be minimized to an insignificant order of appearance. Some of the ejected material can resolidify and accumulate around the hole periphery forming the spatter which is one of the undesirable effects of laser drilling and requires subsequent finishing operations [5]. Innovative laser drilling techniques based on gel casting methods have been developed for reducing the deposition of spatter and strong alumina parts were successfully produced by this technique [6].

Lasers in pulsed mode offer high peak powers in a short time period, increasing thermal impact and enabling drilling through thicker material [1]. Lasers are used for industrial precision drilling for applications such as cooling holes in gas turbine components [7]. Drilling of SiC is particularly interesting to the semiconductor industry for the production of cooling plates. Metals, alloys, organic as well as inorganic nonmetals, ceramics, and composites can be drilled by lasers [8]. Recently, excimer lasers have been widely used for drilling purposes as each pulse eliminates only a thin layer of the material leading to precise control over the drill depth

A. N. Samant · C. Daniel · N. B. Dahotre (✉)
Department of Materials Science and Engineering,
The University of Tennessee,
Knoxville, TN 37996, USA
e-mail: ndahotre@utk.edu

C. Daniel · R. H. Chand · C. A. Blue
Materials Science and Technology Division,
Oak Ridge National Laboratory,
Oak Ridge, TN 37831, USA

and eliminating mechanical impact which poses a particular problem to composites. Nd:YAG lasers have been used for drilling holes in ceramics such as zirconia, which could be used for making ornaments such as necklaces and earrings. The effect of processing parameters on the heat affected zone (HAZ) thickness, and tapering of the holes drilled in zirconia ceramic has been studied [9]. As the ceramics are very brittle, drilling of ceramics is associated with fracture and crack generation [10]. Of the different available ceramics, silicon carbide (SiC) has long been considered as an outstanding material for high temperature, high power, and high frequency applications [11]. Due to its high thermal conductivity, mechanical hardness, excellent chemical resistance, and low thermal expansion coefficient, drilling of SiC is gaining popularity for different industrial needs. Besides Sciti et al. [12], not much work has been reported on the laser drilling of SiC. Hence, the present study aims at understanding the physical phenomena underlying the drilling of SiC ceramic by pulsed Nd:YAG laser and presents a mathematical model for predicting the effect of laser processing parameters on the depth of the drilling hole.

2 Experimental part

Conventional chemical vapor deposited (CVD) silicon carbide plates of 2 and 3 mm thickness were used for the drilling study. A JK 701 pulsed Nd:YAG laser (1064 nm wavelength) from GSI Lumonics, Rugby, England was used to drill SiC plates of 2 and 3 mm thicknesses. The laser had the capabilities to provide repetition rates varying from 0.2 to 500 Hz, pulse energy in the range of 0.1–55 J, and the pulse width ranging from 0.3–20 ms. The laser processing parameters such as peak power, pulse width, and repetition rate were varied in several different combinations until identification of a set of parameters that provided sufficient interaction between the laser beam and the ceramic surface for required through drilling of SiC plates. For this set of laser processing parameters, multiple pulses were applied until a through hole was drilled in SiC plates. It was observed that for a power of 300 W, pulse duration of 0.5 ms, and repetition rate of 50 Hz, a through hole in the 2 mm thick plate could be drilled in approximately 0.5 s, while under the same conditions, a through hole in the 3-mm thick plate was produced in approximately 2.5 s. De-focusing of the laser through a thicker plate decreases the actual fluence (energy density) at the material front, and needed pressure to eject the molten fraction of decomposed species increases with the hole depth, thus leading to a decreased material removal rate while proceeding through the thickness. Therefore, the drilling time is not a linear function of the thickness.

Under the set of parameters employed in the present work, the repetition rate of 50 Hz over 0.5 s corresponded to 25 pulses, while over 2.5 s, it was equivalent to 125 pulses. The visual observations ensured the creation of holes (Fig. 1) with 25 and 125 pulses in 2 and 3 mm thick plates, respectively. As mentioned earlier, these holes were drilled with a lens of longer focal length and longer focal waist to minimize the tapering effect. But experimentally observed prediction of the exact number of pulses required to produce through hole during such laser-based rapid process remains a challenging task. In light of this, development of a computational model for such predictions is the most appropriate approach. Furthermore, the computational model can be extended to predict drilling parameters for plates of other thicknesses. The physical processes taking place along the depth are entirely different from those occurring at the surface. Efforts are ongoing to incorporate them in the computational model which will enable to predict the hole diameter at the surface, and this will be presented in due course of time. However, for the present study, the hole diameter is assumed to be equivalent to the laser-spot diameter [13].

3 Computational approach: temporal evolution, recoil pressure, and surface tension effects

During the drilling process, temperature at the surface of the ceramic changes because of the absorbed laser energy. To predict the depth of drilled hole, the surface temperature profiles and associated thermal gradient within the material were calculated. In order to estimate the temperature rise during the ON time and the following temperature drop during the OFF time, the ON and OFF times during drilling under the present set of laser parameters were calculated and along with the process parameters employed in the present study are represented in Table 1. Table 1 also represents the actual drilling energy required (3.75 J for the 2-mm thick plate and 18.75 J for the 3 mm thick plate), which was calculated by multiplying the power (300 W) by the total ON time (12.5 ms for the 2 mm thick plate and 62.5 ms for the 3 mm thick plate).

The computations were run until the hole was drilled through the entire thickness of the plate (2 and 3 mm) and were started with calculation of the maximum temperature reached after the first pulse employing a three-dimensional heat transfer flow model which was developed in COMSOL's heat transfer mode [14] and was based on Fourier's second law of heat transfer:

$$\frac{\partial T(x,y,z,t)}{\partial t} = \frac{k(T)}{\rho C_p(T)}\left[\frac{\partial^2 T(x,t)}{\partial x^2} + \frac{\partial^2 T(y,t)}{\partial y^2} + \frac{\partial^2 T(z,t)}{\partial z^2}\right] \quad (1)$$

where $k(T)$ and $C_p(T)$ are the variations in thermal conductivity and specific heat as a function of temperature,

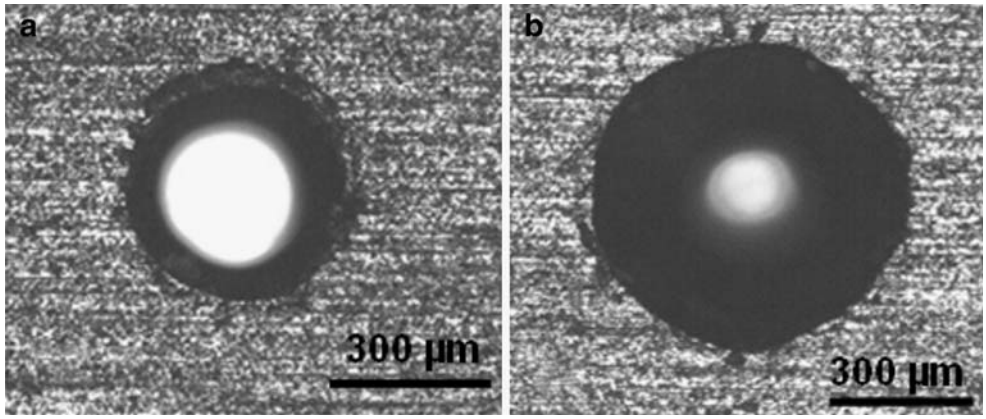

Fig. 1 Front surface showing drilled holes in **a** 2 mm and **b** 3 mm SiC plates

ρ is the density of SiC (3,100 kg/m^3) [15], T is the temperature field, t is time, and x, y, and z are the spatial directions. For improving the accuracy of calculations, variation of thermal conductivity and specific heat as a function of temperature (Fig. 2) were taken into account in the model, and these properties were assumed to be constant after about 1,700 K [15] The latent heat of solidification was accounted for by considering the variation of specific heat as a function of temperature. At time t=0, the initial temperature of T=T_0=300 K was applied. The balance between the absorbed laser energy at the surface and the radiation losses was given by:

$$-k(T)\left(\frac{\partial T(x,y,0,t)}{\partial x}+\frac{\partial T(x,y,0,t)}{\partial y}+\frac{\partial T(x,y,0,t)}{\partial z}\right)=\delta \mathrm{al}-\varepsilon\sigma\left(T(x,y,0,t)^4-T_0^4\right)$$
$$\delta=1 \quad \text{if } 0\le t\le t_{\mathrm{on}}$$
$$\delta=0 \quad \text{if } t>t_{\mathrm{on}} \tag{2}$$

where $k(T)$ is the temperature dependent thermal conductivity of the material (W/mK), ε is emissivity for thermal radiation (0.7) [15], I is the laser power intensity, t_{on} is the ON time, σ is Stefan–Boltzman constant (5.67×10^{-8} W/m^{2}K^4), and a is the absorptivity of the material. The term δ takes a value of 1 when the time, t, is less than the pulse on-time, t_{on}, and it is 0 when the time, t, exceeds the pulse on-time. Thus, the value of δ depends on the time, t, and ensures that the energy is input to the system only during the pulse on-time and cuts off the energy supply during the following pulse off-time.

SiC has a very high absorptivity of 0.95 at 1,064 nm wavelength (for Nd:YAG laser used in present case) and 1,298 K [15], and this value increases with temperature as the depth of the drilled hole increases. The drilled hole is partially filled with decomposed liquid and vapor species, and the laser beam undergoes multiple reflections and absorption within the cavity and these phases (melt and vapor species) for increased absorption of laser energy. Due to a very high absorptivity of SiC (0.95) coupled with further increased absorption due to these physical changes within the laser–substrate interaction region, the resultant absorption of the ceramic is almost instantaneously expected to reach nearly 100%. Earlier, similar explanations and assumptions during laser processing of a variety of materials are adopted [16, 17]. Furthermore, for an extremely short duration, high-energy density dynamic process like laser–material interaction, it has been extremely difficult to accurately conduct in situ measurements for the instant at which the ceramic starts absorbing all the input energy. In light of this, in the present study, it was reasonable to consider the drilled hole as a black body with 100% absorption. The convection taking place at the bottom surface of the sample was given by:

$$-k(T)\left(\frac{\partial T(x,y,L,t)}{\partial x}+\frac{\partial T(x,y,L,t)}{\partial y}+\frac{\partial T(x,y,L,t)}{\partial z}\right)=h(T(x,y,L,t)-T_0), \tag{3}$$

where L is the thickness of the sample which was taken as 2 and 3 mm for the two different SiC plates used in the present study, and h is the heat transfer coefficient (W/m^{2}K) which was included as a function of temperature [18]. In the short time scale used for laser processing, the heat flow in the direction orthogonal to the laser beam can be neglected. Thus, Eqs. 1, 2, and 3, above could be considered to represent the heat flow, radiation losses, and

Table 1 Parameters for laser processing

Plate thickness (mm)	Operation time (s)	Number of pulses	Drilling energy (J)	Pulse width (ON time) (ms)	OFF time (ms)	Total ON time (ms)	Total OFF time (ms)
2	0.5	25	3.75	0.5	19.5	12.5	487.5
3	2.5	125	18.75	0.5	19.5	62.5	2437.5

convection, respectively, taking place only along the z direction, neglecting these phenomena in the x and y directions. Incorporation of these effects in the x and y directions will be dealt in subsequent work and will be presented in the future. The solution of this model gave the maximum surface temperature reached after the first pulse which was input in Eq. 4, below to predict the temperature reached after the laser is switched off [2]:

$$T_i^{'} = T_i + (T_0 - T_i)\left[1 - \left[\exp\frac{h(T)^2\alpha(T)t_{\text{off}}}{k(T)^2}\right]\left[1 - \text{erf}\left(\frac{h(T)\sqrt{\alpha(T)t_{\text{off}}}}{k(T)}\right)\right]\right] \quad (4)$$

where T_i is the temperature during heating of pulse i (K), T_0 is the ambient temperature of 300 K, t_{off} is the OFF time between successive pulses (Table 1) and erf() is the error function. The term $\alpha(T)$ is the temperature-dependent thermal diffusivity of the material given by $k(T)/\rho C_p(T)$. When the laser is active, the surface temperature is given by [2]:

$$T_i = T_{i-1}^{'} + \frac{8\text{aP}}{\pi \text{d}^2}\frac{\sqrt{\alpha(T)t_{on}/\pi}}{k(T)} \quad (5)$$

where $T_{i-1}^{'}$ is the temperature during cooling of the earlier pulse (K) predicted from Eq. 4, above, a is the absorptivity of the material mentioned above, P is the incident beam power (300 W), d is the beam diameter (0.24 mm), and t_{on} is the pulse duration (ON time). The temperatures reached during the ON and OFF periods of the successive pulses were determined by repeatedly solving Eqs. 4 and 5, until the thickness of the plate was reached. The expressions for the temperatures reached during the ON and OFF periods (Eqs. 4 and (5), above) were valid as the heat transfer occurring in the direction perpendicular to the laser beam was not considered. As mentioned above, the processing time being extremely small, these assumptions were justified.

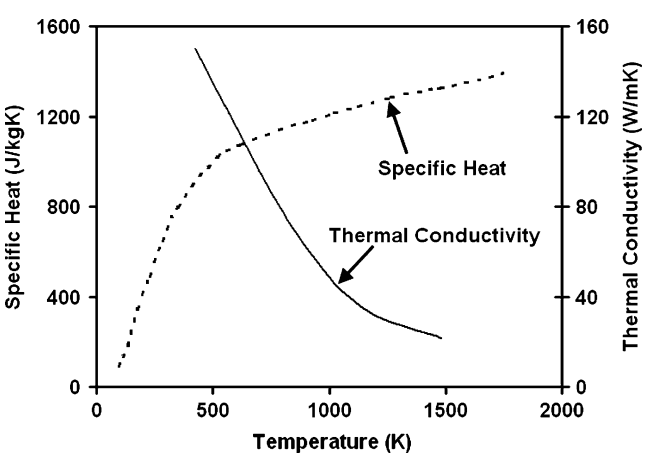

Fig. 2 Variation of thermophysical properties with temperature [15]

The decomposition temperature of SiC is 3,103 K [19] at which decomposition products immediately melt. The melt depth (z_t) from the surface at any instant was predicted from the temperature profiles by tracking the depth at which this decomposition temperature was reached. This depth was used as a starting point for further calculations. However, there was some loss of material at the surface due to evaporation and the rate of evaporation j_d (kg/m^{2}s) [20] is given by:

$$j_d = p(T_\text{s})\left[\frac{m_\text{v}}{2\pi k T_\text{s}}\right]^{1/2} \quad (6)$$

where m_v is mass of the vapor molecule (6.641×10^{-26} kg/at for SiC), T_s is the surface temperature, k is the Boltzmann constant (1.38065×10^{-23} J/K), and $p(T_\text{s})$ is the saturation pressure given by the Clausius–Clapeyron equation:

$$p(T_\text{s}) = p_0 \exp[(L_v/kT_\text{e})(1 - T_\text{e}/T_\text{s})] \quad (7)$$

where p_0 is the ambient pressure (1.013×10^5 N/m^2), L_v is latent heat of evaporation (530 kJ/mol for SiC) [21], and T_e is the evaporation/decomposition temperature. The equivalent depth of material evaporated was predicted from the rate of evaporation by the relation:

$$z_\text{eva} = \frac{j_d \times \text{increment in time}}{\rho} \quad (8)$$

where ρ is the constant value of density of SiC (3,100 kg/m^3) [15] mentioned above, and this evaporated depth (z_eva) (Fig. 3) was subtracted from the melt depth (z_t) to give the

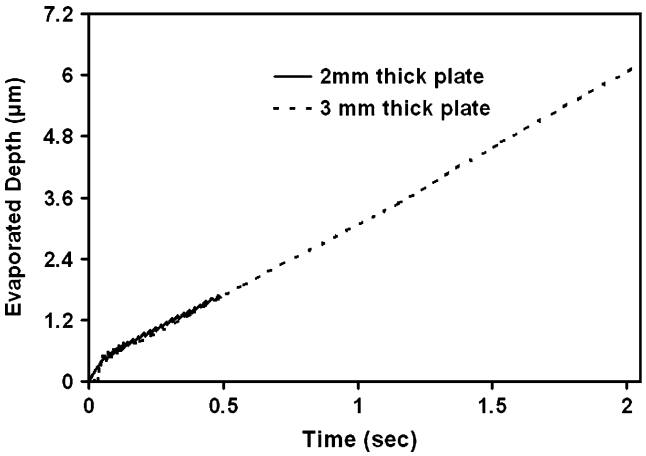

Fig. 3 Material evaporation with time for SiC drilling

available melt pool (z_{ava}). The amount of material evaporated increased with time, as it depends on the surface temperature which also increased with time during the ON time of each pulse. At the same time, there is a drop in temperature at any instant at the surface due to cooling of the melt pool by evaporation which is predicted by [22]:

$$\Delta T_{eva} = \frac{2 z_{eva} \rho L_v}{k(T) t\, d \pi^{3/2}} \operatorname{arc\,tg} \frac{4\sqrt{\alpha(T) \times \text{increment in time}}}{d} \tag{9}$$

where z_{eva} is the depth of material evaporated as predicted from Eq. 8, above, $k(T)$ is the temperature dependent thermal conductivity of the material (W/mK) [15] mentioned above, and the term $\alpha(T)$ is the temperature dependent thermal diffusivity of the material given by $k(T)/\rho C_p(T)$. This drop in temperature was subtracted from the temperature predicted by Eqs. 4 and 5 above to give the actual surface temperature at any given time instant as represented in Fig. 4. The heating curve meanders because the temperature drops during the OFF time and rises during the ON time of the laser even after a drop due to the evaporation. The maximum surface temperature reached, while drilling the 2-mm thick plate was more compared to the maximum surface temperature reached for drilling through the 3-mm thick plate as more number of pulses (more time) were required for drilling through the 3-mm plate compared to the 2-mm thick plate.

Depending upon the thermodynamic conditions prevailing during laser drilling, the decomposition of SiC may produce several stoichiometric and/or nonstoichiometric species such as $Si_{(l)}$, $C_{(s)}$, $C_{(g)}$, $Si_{(g)}$, $Si_{3(g)}$, $Si_{2(g)}$, $SiC_{2\ (g)}$, $Si_2C_{(g)}$, and $Si_{(s)}$ [12]. In situ detection of formation of these species during extremely dynamic and short duration laser drilling process is a challenging task and will be considered in future efforts. However, the most likely reaction to produce liquid species at the decomposition temperature is the following reaction.

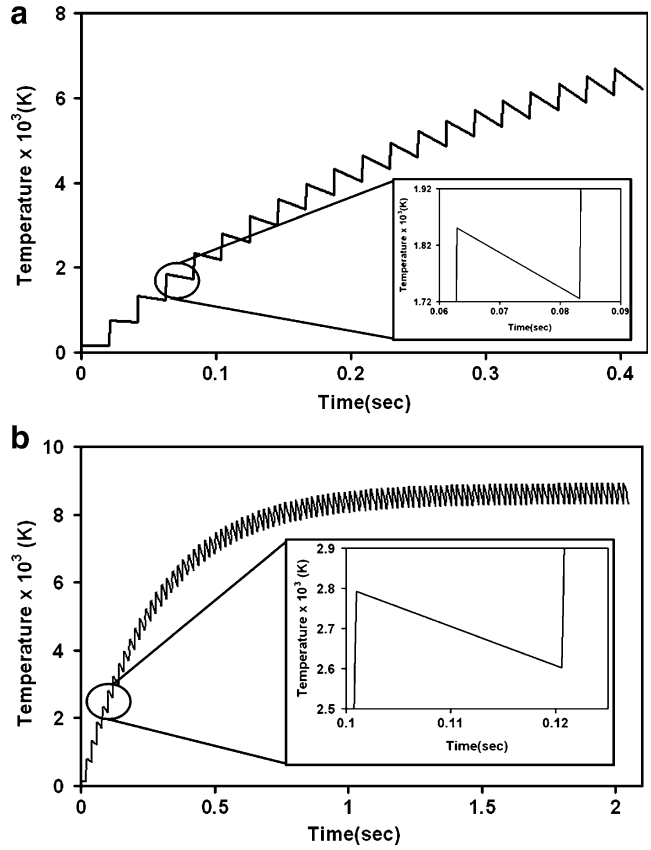

Fig. 4 Heating curves for **a** 2 mm thick plate and **b** 3 mm thick plate

$$SiC = Si_{(l)} + C_{(s)} \tag{10}$$

The Gibbs free energy associated with this reaction (−335.96 kJ/mol at 3259 K [23]) was used to determine the energy loss due to dissociation. Due to the presence of a minimum taper as mentioned above, the hole could be assumed to have a cylindrical cross section (of volume $V_{pool} = \frac{\pi\left(0.24\times10^{-3}\right)^2 z_{ava}}{4}\,m^3$. As 1 mol of a substance corre-

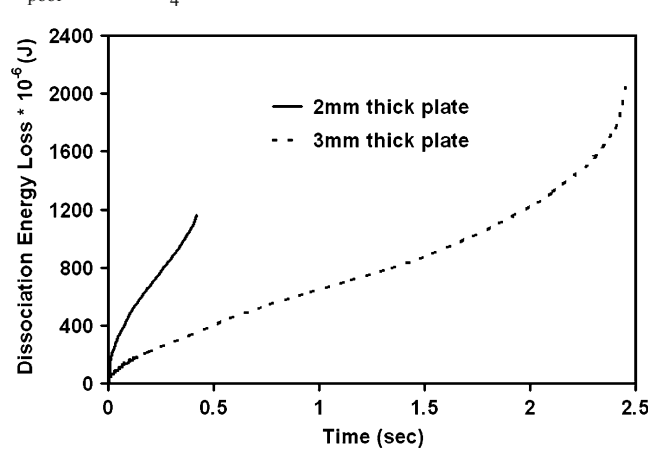

Fig. 5 Dissociation Energy loss during SiC drilling

sponds to 22.4×10^{-3} m^3, there will be $2.019\times10^{-6}\times z_{ava}$ moles in the volume V_{pool} of the melt and the energy loss due to dissociation (Fig. 5) is expressed as

$$E_{diss} = (0.6783 \times z_{ava})J \tag{11}$$

This energy loss was subtracted from the input laser energy to give the effective laser energy for subsequent pulses. The dissociation energy losses increased with time, as it was a function of the melt depth which also increased with time.

The ejection of the molten material can take place either by the reactive recoil pressure due to the vapor or plasma of the ambient medium and cannot take place by both the mechanisms. At laser intensities of the order of 10^9 W/cm, the purely evaporational mechanism of material removal takes place [24]. Thus the mechanism for material removal is dictated by the laser beam intensity. However, for an incident beam power of 300 W and beam diameter of 0.24 mm used in the present study, the laser intensity was 1.25×10^4 W/cm which was far less than the intensity required for the plasma pressure effect on material removal. Hence, the effect of plasma pressure was neglected and only the effect of evaporation induced recoil pressure on material removal was considered.

As mentioned earlier, a melt pool comprising of liquid Si produced due to the decomposition of SiC during the laser irradiation is formed below the vaporization front, and the expulsion of this molten material at very high velocities is driven by the recoil pressure stimulated by some of the decomposed species [25, 26]. However, the entire melt pool measured from the surface was not available for expulsion. Only the portion remaining after a fraction of the available melt depth (z_{ava}) was expelled by the recoil pressure would be the effective melt depth (z_{eff}), and it will be available for expulsion for the next time instant. The fraction of the melt pool that is expelled by the recoil pressure will be predicted in the later part of this section. The evaporation-induced recoil pressure p_r is given by [27]:

$$\frac{\pi d^2 p_r}{4aP} = \frac{1.69}{\sqrt{L_v}}\left(\frac{b}{1+2.2b^2}\right) \tag{12}$$

where $b^2 = kT_s/m_v L_v$. Thus, the predicted temperature field assisted in determining the evaporation-provoked recoil pressure at the surface during drilling through the SiC ceramic using the physical model of melt hydrodynamics proposed by Anisimov who also experimentally verified the same [27]. According to Anisimov, when the surface temperature exceeds the boiling point or the decomposition temperature, the recoil pressure becomes $0.55p_s$, where p_s is the saturated vapor pressure (1.01325×10^5 N/m^2). Under typical materials processing conditions such as those encountered in drilling, this recoil pressure exceeds the highest surface tension pressure and plays a vital role in removal of material in molten state.

It can be seen from the heating curves shown above in Fig. 4 that the maximum surface temperature reached for drilling through the entire depth of 3 mm plate was more than that reached while drilling through the 2-mm plate. However, the maximum recoil pressure attained (Fig. 6) was almost the same for both the cases (~3.73×10^5 Pa). It can be observed from Eq. 12 that the recoil pressure depends not only on the maximum surface temperature but also on the laser power which was the same in both the cases (300 W). The recoil pressure does not continuously increase with surface temperature. Once a certain maximum surface temperature was reached after some pulses and the corresponding maximum recoil pressure was attained, then the recoil pressure ceases to increase any further. After the maximum recoil pressure was reached, even though there was a slight drop in the recoil pressure, it was sufficient to continue expulsion of the fraction of the molten part of the decomposed species available at different time instants.

The melt pool shape is affected by the surface tension in addition to the presence of recoil pressure [28]. It was necessary to consider the surface tension effect, as it modifies the pressure on the melt and affects the depth of the drilled hole. The surface tension pressure depends on the effective beam radius [25], which changes as it gets defocused with the changes in the hole depth and is given by [2]:

$$r_{eff} = \frac{d}{2}\left[1+\left(M^2\frac{4\lambda(Z_{eff}+\delta_f)}{\pi d^2}\right)^2\right]^{1/2} \tag{13}$$

where λ is the laser wavelength (1,064 nm), δ_f is the focal length (120 mm), M^2 is the beam quality parameter assumed to be 1 for a perfect Gaussian beam profile, and z_{eff} is the effective melt depth explained earlier. Beam

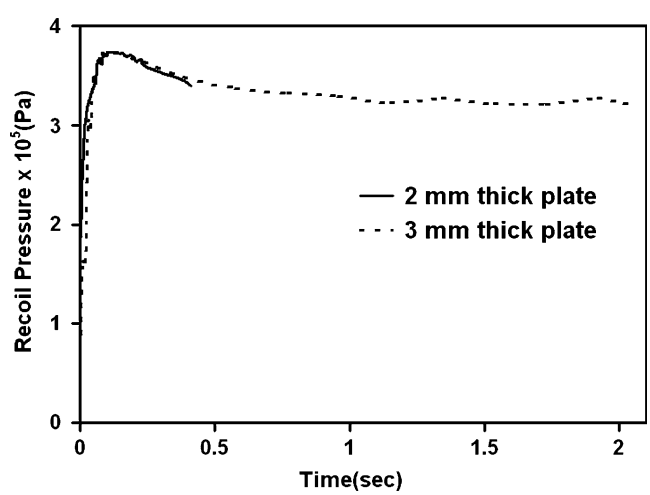

Fig. 6 Recoil pressure variations with time for SiC drilling

quality is a measure of the focusability of the laser used, and beam quality factor is a standard measure used for the same. In this study, it is assumed that the beam is initially at full focus corresponding to a beam quality factor of 1. All real beams tend to have an M^2 value greater than 1. Attempts are ongoing for accurate M^2 determination, and they will be incorporated in future work. However, the effect of the defocusing of the laser beam is taken into account by determining the effective beam radius from Eq. 13 above. The melt available at the axis of the beam was expelled with a velocity $v_{\exp}$ given by [25]:

$$v_{\exp}(t) = \frac{1}{\rho}\frac{p_{\mathrm{r}} - \tau/r_{\mathrm{eff}}}{r_{\mathrm{eff}}}t \tag{14}$$

where r_{eff} is the effective beam radius determined above in Eq. 13, t is the time, and τ is the surface tension coefficient. As the thermophysical properties of SiC control the dissociation of SiC into its species, the SiC properties were considered only until SiC dissociated into liquid Si after which the properties of Si melt were taken into account. Hence, the surface tension coefficient of liquid Si (843 dyne/cm for liquid Si [29]) was considered as it affects the expulsion velocity and hence the depth of the drilled hole. The fraction of the effective melt depth that was expelled at a certain time instant, d_t, was obtained by integrating the expelled velocity over time (Eq. 15) and the depth of the hole was given by Eq. 16 [30],

$$d_t = \int_0^t v_{\exp}(t)\,d\,t \tag{15}$$

$$h_t = \sum_0^t d_t \tag{16}$$

The step-wise procedure followed to achieve the final depth is presented in Fig. 7, where it can be seen that the material properties and dimensions along with the laser processing parameters were used to solve the fundamental heat transfer equation to obtain the preliminary temperature profiles and melt depth predictions. The input energy, melt depth, and heating curves were altered due to the losses taking place during the dissociation and evaporation processes. The modified temperature profiles then assisted in determining the recoil pressure and associated velocity of expulsion of the melt leading to the final determination of the hole depth and prediction of required number of pulses. The evolution of the drilled hole with time and the different stages of its formation are schematically represented in Fig. 8a, b, respectively.

It can be observed from Fig. 8a that a 2-mm thick plate was drilled through its entire depth in 0.41 s, while it took 2.05 s to drill through the entire thickness of a 3-mm thick plate. Thus, only 21 pulses for a 2-mm plate and 103 pulses for a 3-mm plate were required to drill through the entire thickness. The predicted total ON time (for a pulse duration of 0.5 ms) corresponding to 21 pulses and 103 pulses was 10.5 and 51.5 ms, respectively. The corresponding predicted drilling energy was obtained by multiplying the power (300 W) by the total predicted ON times for the 2 and 3 mm thick plates, and these drilling energies have also been compared in Table 2. Therefore, as can be seen from Table 2, computationally predicted number of pulses and drilling energy was less than those experimentally identified [25 pulses (3.75 J) for the 2 mm plate and 125 pulses (18.75 J) for the 3-mm plate]. This discrepancy is due to the fact that selection of number of pulses during actual drilling was based on prior practical experience in laser–materials interactions and visual observations. It can be observed from Fig. 8b that in the initial stages of drilling (until around time instant t_2), the recoil pressure expelled the material in the upward direction and continued to do so for increased depth of the drilled hole as the time progressed. Eventually, when a

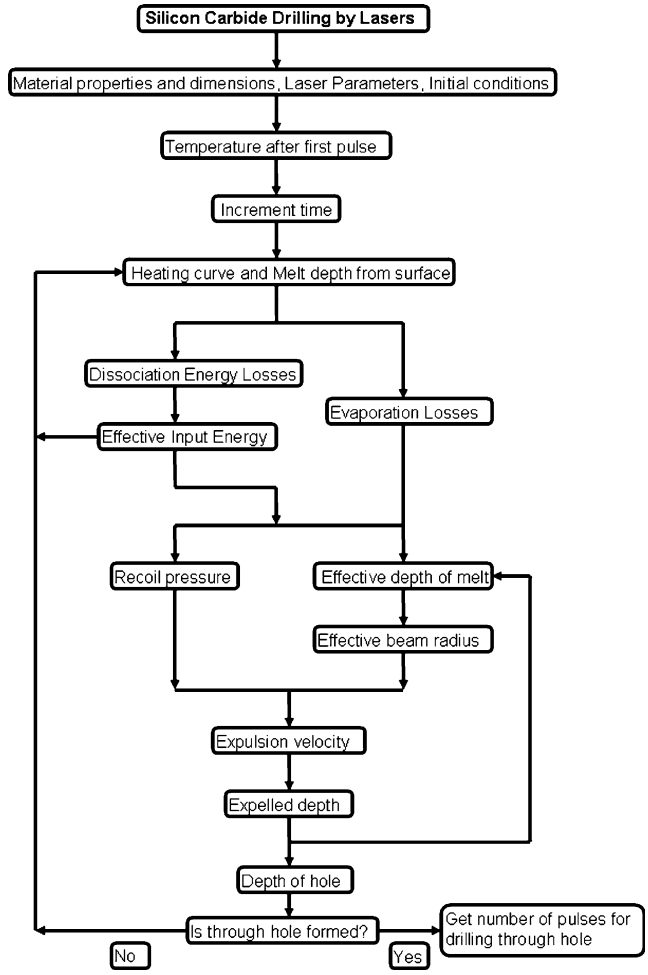

Fig. 7 Flowchart showing procedure for prediction of drilled depth

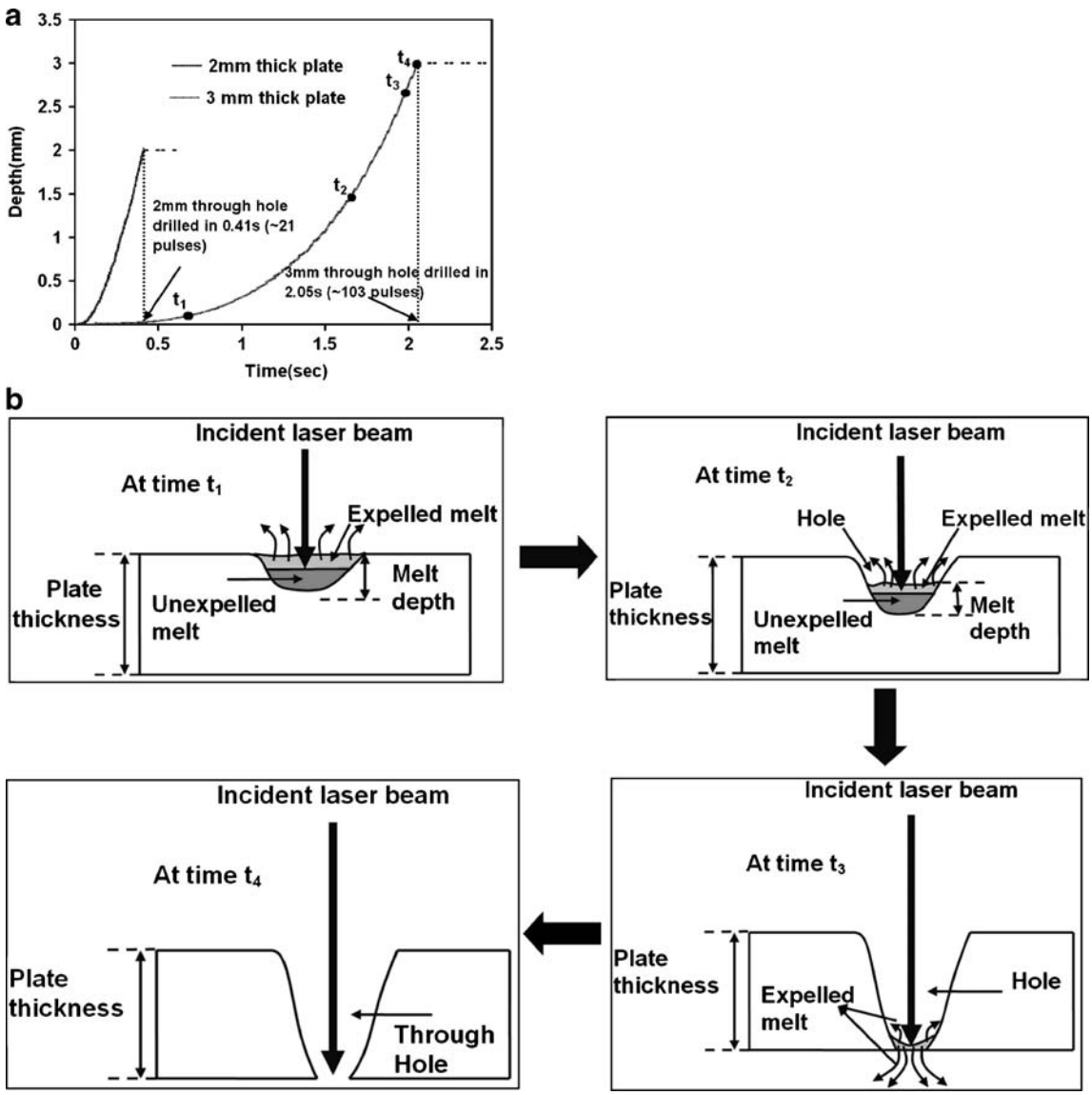

Fig. 8 **a** Evolution of drill depth with time. **b** Schematic for progression of hole formation during through drilling of ceramic

very thin layer of the material remained in the bottom (at around time instant t_3), the recoil pressure was able to push most of the material in the downward direction thereby reversing the direction of material expulsion in the final stages of drilling. This happened due to the least resistance to the recoil pressure by the small mass of supporting material at the bottom. Finally, at around time instant t_4, all the rest of molten material was expelled and a clean through hole was formed. Thus, the prediction of exact number of pulses (for that matter pulse duration, laser energy, etc.) to drill a required depth in a given type of material under chosen set of laser processing parameters would be extremely advantageous to conserve substantial energy and time.

Table 2 Comparison between measured and predicted number of pulses and drilling energy

Plate thickness (mm)	Number of pulses$_{measured}$	Number of pulses$_{predicted}$	Drilling energy$_{measured}$ (J)	Drilling energy$_{predicted}$ (J)
2	25	21	3.75	3.15
3	125	103	18.75	15.45

4 Conclusion

Through drilling of silicon carbide was successfully carried out using pulsed Nd:YAG laser. A comprehensive theoretical model incorporating the thermal effects in decomposing material, the effect of evaporation induced recoil pressure, surface tension in expelling molten part of the decomposed species, cooling of the surface due to evaporation, and loss in energy due to dissociation assisted in prediction of a drill depth under given processing conditions. Such comprehensive approach distinguished the model from many earlier works including that of Salonitis et al. [2] who considered the drilling mechanism as the melting and subsequent removal of a material volume and Sciti et al. [12] who only considered the microstructural surface modification of SiC as a function of laser processing parameters without considering the actual physical phenomena such as the effect of recoil pressure, evaporation losses, and dissociation energy losses responsible for hole formation as considered in the present study.

In the present study, the computational model specifically indicated that although 25 pulses (3.75 J) and 125 pulses (18.75 J) were employed, only 21 pulses (3.15 J) and 103 pulses (15.45 J) were sufficient for drilling through the entire thickness of 2 and 3 mm plates, respectively, under the present laser processing conditions. The maximum recoil pressure of ~3.73×10^5 Pa predicted by the model was responsible for expulsion of the melt pool during drilling. Even though the loss of material due to evaporation at the surface contributed to only a small fraction of the total depth drilled through the SiC plate, it was essential to be considered as its magnitude depends on the thermophysical properties of the material and the processing conditions, and these losses could be significant in the drilling of some other materials. Thus, the model is capable of providing an advance estimate of the number of pulses required to drill a desired depth in a given material.

Acknowledgement Claus Daniel acknowledges financial support from the Eugene P. Wigner Fellowship Program at Oak Ridge National Laboratory, managed by UT-Battelle, LLC, for the U.S. Department of Energy under contract no. DE-AC05-00OR22725.

References

1. Dubey AK, Yadava V (2008) Experimental study of Nd:YAG laser beam machining—an overview. J Mater Process Tech 195:15–26. doi:10.1016/j.jmatprotec.2007.05.041
2. Salonitis K, Stournaras A, Tsoukantas G, Stavropoulos P, Chryssolouris G (2007) A theoretical and experimental investigation on limitations of pulsed laser drilling. J Mater Process Tech 183:96–103. doi:10.1016/j.jmatprotec.2006.09.031
3. Srinivasa MJ (1994) Investigation of the drilling dynamics and melt expulsion mechanisms during the laser drilling of Ti-6Al-4V using high speed photography Masters Thesis University of Tennessee
4. Ghoreishi M, Low DKY, Li L (2002) Comparative statistical analysis of hole taper and circularity in laser percussion drilling. Int J Mach Tools Manuf 42:985–995. doi:10.1016/S0890-6955(02)00038-X
5. Low DKY, Li L, Byrd PJ (2003) Spatter prevention during the laser drilling of selected aerospace materials. J Mater Process Tech 139:71–76. doi:10.1016/S0924-0136(03)00184-5
6. Guo D, Cai K, Yang J, Huang Y (2003) Spatter-free laser drilling of alumina ceramics based on gelcasting. J Eur Ceram Soc 23:1263–1267. doi:10.1016/S0955-2219(02)00299-6
7. Yeo CY, Tam SC, Jana S, Lau MWS (1994) A technical review of the laser drilling of aerospace materials. J Mater Process Tech 42:15–49. doi:10.1016/0924-0136(94)90073-6
8. Meijer J (2004) Laser beam machining (LBM), state of the art and new opportunities. J Mater Process Tech 149:2–17. doi:10.1016/j.jmatprotec.2004.02.003
9. Kuar AS, Doloi B, Bhattacharyya B (2006) Modelling and analysis of pulsed Nd:YAG laser machining characteristics during micro-drilling of zirconia (ZrO2). Int J Mach Tools Manuf 46:1301–1310. doi:10.1016/j.ijmachtools.2005.10.016
10. Nedialkov N, Sawczak M, Jendrzejewski R, Atanasov P, Martin M, Śliwiński G (2007) Analysis of surface and material modifications caused by laser drilling of AlN ceramics. Appl Surf Sci 254:893–897. doi:10.1016/j.apsusc.2007.07.151
11. Zoppel S, Farsari M, Merz R, Zehetner J, Stangl G, Reider GA et al (2006) Laser micro machining of 3C–sic single crystals. Microelectron Eng 83:1400–1402
12. Sciti D, Bellosi A (2001) Laser-induced surface drilling of silicon carbide. Appl Surf Sci 180:92–101. doi:10.1016/S0169-4332(01)00330-0
13. Ng GKL, Crouse PL, Li L (2006) An analytical model for laser drilling incorporating effects of exothermic reaction, pulse width and hole geometry. Int J Heat Mass Transfer 49:1358–1374. doi:10.1016/j.ijheatmasstransfer.2005.10.002
14. Harimkar SP, Samant AN, Dahotre NB (2007) Temporally evolved recoil pressure driven melt infiltration during laser surface modifications of porous alumina ceramic. J Appl Phys 101:054911.1–054911.7. doi:054911
15. Touloukian YS (1967) Thermophysical Properties of High Temperature Materials. IFI/Plenum, New York
16. Andrews JG, Atthey DR (1976) Hydrodynamic limit to penetration of a material by a high-power beam. J Phys D Appl Phys 9:2181–2194. doi:10.1088/0022-3727/9/15/009
17. Mazumdar J, Steen WM (1980) Heat transfer model for cw laser material processing. J Appl Phys 51:941–947. doi:10.1063/1.327672
18. Incropera FP, Dewitt DP (2002) Fundamentals of heat and mass transfer. Wiley, New York
19. Bhushan B, Gupta BK (1991) Handbook of Tribology Materials, Coatings and Surface Treatments. Mc Graw Hill, New York
20. Duley WW (1998) Laser welding. Wiley, New York, NY
21. Reitano R, Baeri P (1996) Nanosecond laser-induced thermal evaporation of silicon carbide. Int J Thermophys 17:1079–1087. doi:10.1007/BF01441996
22. Allmen MV, Blaser P, Affolter K, Strumer E (1978) Absorption phenomena in metal drilling with Nd-lasers. IEEE J Quantum Electron 14:85–88. doi:10.1109/JQE.1978.1069739
23. Barin I, Knacke O (1973) Thermochemical properties of inorganic substance. Springer, New York
24. Anisimov VN, Arutyunyan RV, Baranov VY et al (1984) Applied Optics 23:18–24

25. Matsunawa A, Semak V (1997) The simulation of front keyhole wall dynamics during laser welding. J Phys D Appl Phys 30:798–809. doi:10.1088/0022-3727/30/5/013
26. Semak V, Matsunawa A (1997) The role of recoil pressure in energy balance during laser materials processing. J Phys D Appl Phys 30:2541–2552. doi:10.1088/0022-3727/30/18/008
27. Anisimov SI (1968) Vaporization of metal absorbing laser radiation. Sov Phys JETP 27:182–183
28. Han L, Liou FW, Musti S (2005) Thermal behavior and geometry model of melt pool in laser material process. J Heat Transf 127:1005–1014. doi:10.1115/1.2005275
29. Yuan ZF, Mukai K, Huang WL (2002) Surface temperature and its temperature coefficient of molten silicon at different oxygen potentials. Langmuir 18:2054–2062
30. Semak VV, Knorovsky GA, MacCallum DO, Roach RA (2006) Effect of surface tension on melt pool dynamics during laser pulse interaction. J Phys D Appl Phys 39:590–595. doi:10.1088/0022-3727/39/3/025